Aerodynamic performance of flying discs

KAMARUDDIN, Noorfazreena M., POTTS, Jonathan R. <http://orcid.org/0000-0001-8192-0295> and CROWTHER, William J.

Published version

KAMARUDDIN, Noorfazreena M., POTTS, Jonathan R. and CROWTHER, William J. (2018). Aerodynamic performance of flying discs. Aircraft Engineering and Aerospace Technology, 90 (2), 390-397.

Aerodynamic Performance of Flying Discs

Abstract

Purpose – The purpose of this paper is to examine geometrical design influence of various types of flying discs on their flight performance from the aerodynamics perspective.

Design/methodology/approach – The lift, drag, and moment coefficients of the discs were measured experimentally using a wind tunnel. Three types of golf discs and four sets of simpler parametric discs were studied to analyze and isolate the effect of design factors on these aerodynamic characteristics. Full six degree-of-freedom simulations of the discs were performed to visualize their flight trajectories and attitudes. These simulations, combined with the experimental data, provide details on the well-known "S-shaped" ground-path traced by a flying disc.

Findings – This study reveals two key parameters to evaluate the flight performance of a disc: its coefficient of lift-to-drag ratio (C_L/C_D) and, more importantly, its coefficient of pitching moment (C_M). The latter influences the tendency of the disc to yaw from its intended path, and the former influences its throwing distance.

Practical implications – The work suggests that, to optimize the flight performance of a disc, the magnitudes and gradient of its C_M should be minimized and its trim-point shifted from origin, while its C_L/C_D should be maximized with a flatter peak.

Originality/value – In this study, the design parameters and the aerodynamic characteristics of various types of flying discs are analysed, compared and discussed in depth. Recommendations of design improvements to enhance the performance of any flying disc are offered as well.

Keywords Aerodynamic, Flying disc, Flight Performance.

Paper type *Research paper*

Introduction

The performance of a flying disc, such as a golf disc, is typically measured in terms of its flight range and throwing accuracy. Understanding the effect of design on the flight performance of a disc is crucial for a player to choose the correct disc to throw, and for a manufacturer to improve its design. Although a golf disc is well known as a sport object, it can be characterized as a low aspect ratio wing. This paper investigates the relationship between geometric shape and performance of golf discs, supported by empirical data and numerical simulations to improve the disc design. The flight performance of a disc is governed by its aerodynamic characteristics, influenced by its geometrical properties, e.g.,

camber, rim edge-shape profile, lower-surface cavity height, and thickness-to-diameter ratio. Except for the cavity, the other parameters are familiar design variables of a wing of an aircraft.

Golf discs can be categorised into three types: ‘putter’, ‘mid-range’ and ‘driver’ discs, each associated with its short (<50 m), medium and long (>75 m) flight range, respectively. In general, for a given diameter around 0.2 m, the putter disc has the largest thickness (resulting in the largest frontal area), the largest cavity height, the most rounded rim, and the most cambered top surface. The driver disc lies on the other extreme (e.g., the smallest cavity height and the sharpest rim edge), resulting in the smallest frontal area. The design characteristics and performance of a mid-range disc is transitional between those of the putter and driver discs.

An early work to understand the characteristics of a flying disc through governing mathematical equations and dynamic stability analyses was performed by Lissaman (1998). The biomechanics of throwing a flying disc, particularly the Frisbee disc, were comprehensively studied by Hummel and Hubbard (2001) to examine its effect on the resulting flight patterns. Detailed wind tunnel experiments and numerical simulations on the Frisbee disc have been conducted by Potts and Crowther (2001, 2002) to map its aerodynamic characteristics and predict its flight path. The earliest work on golf discs were investigated by Higuchi *et al.* (2000), using flow visualization to study trailing vortices on a putter disc. Field tests were later conducted (Lissaman and Hubbard, 2010) to measure the flight range of golf discs to maximize their performance. The lack of aerodynamic data of the discs unfortunately prevents further analysis to improve their performance.

In general, conducting performance analyses on sports objects (or implements) require one to identify and establish their influencing parameters (Hughes and Bartlett, 2002). In the case of sports with flying implements, their aerodynamic data are important (Hughes, 2004). For instance, the aerodynamic database for footballs developed by Asai *et al.* (2007) have been used widely to understand its fundamental principles and ultimately improve its performance (Nevill *et al.*, 2008; Passmore et al., 2008). Other sports implements with well-established aerodynamic database are tennis balls (Haake *et al*., 2007), baseballs (Mehta,2008; James and Haake, 2008) and golf balls (Wesson, 2009).

This work establishes aerodynamic data for a set of parametric discs and the three categories of golf discs, obtained from wind tunnel experiments. Their flight path and performance are then analysed through three-dimensional numerical simulations. Results on the parametric discs are analysed to isolate the influence of specific design features on the aerodynamic characteristics of the discs.

Methods

Experiments

Wind tunnel experiments were performed on three golf discs, seven parametric discs, and two baseline discs to measure their aerodynamic forces and moments. The tests were conducted using the open-circuit low-speed Project Wind Tunnel at The University of Manchester, with a 0.9 m x 1.1 m octagonal test section, a maximum speed of 50 m/s, a turbulence level of 0.5%, equipped with a six-component overhead balance. The disc models were mounted vertically on a horizontal axle supported by a vertical strut. To maintain consistency in the results, the discs were tested at a fixed Reynolds number of 3.78×10^5 corresponding to a speed range between 22 m/s to 27 m/s dependant upon the diameters of the discs. The angle of attack (α) ranged from -5^o to 15^o, taken at 1^o increment. The measured parameters were the lift and drag forces of the discs (errors within 0.01 N), and the pitching moment about the centre of the disc (errors within 0.001 Nm); these data were normalized into the coefficients of lift (C_L), drag (C_D), and pitching moment (C_M). The side force and the yawing and rolling moments were negligible for the range of α tested, as expected for a non-spinning disc. The spin-dependent changes in the aerodynamic loads were also negligible (Potts, 2005).

Parametric discs

A number of disc models were fabricated with varying geometric properties to parametrically isolate their effect on the aerodynamic characteristics of the discs. Three groups of these parametric models are presented in this paper, with the following geometric variations: camber ratio, defined as the ratio between the difference of the centre-to-rim height (h) and the thickness (t) of the disc; cavity ratio, defined as the ratio between the cavity height (h_c) and the thickness of the disc, and the rim edge-shape profile. The discs were manufactured using Acrylinitrile Butadiene Styrene plastic material, each with a diameter (d) of 0.2 m and a thickness-to-diameter ratio (t/d) of 0.1. A flat disc with identical thickness-to-diameter ratio and square rim edge-profile was tested as the reference baseline data.

Golf discs

Off-the-shelf commercial golf discs were tested: the Aviar^{TM} putter disc, the Roc^{TM} mid-range disc, and the Wraith^{TM} driver disc; all were designed with cavities (Figure 1). These plastic models were modified from their original forms: the thin-wall upper surface of each disc was reinforced underneath with a layer of carbon fibre to prevent any deformation during the wind-tunnel experiments. Comparisons were made with a thinner flat disc (t/d = 0.01) and a Frisbee disc (t/d = 0.14) from the work of Potts and Crowther (2002).

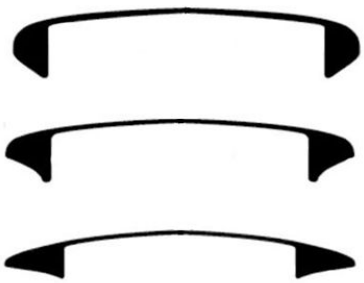

Figure 1 Commercial golf discs tested in the wind tunnel; Putter 'Aviar ™'(top), Mid-range 'Roc™' (middle) and Driver 'Wraith ™' (bottom).

Simulation

A full six degree-of-freedom model of the flights of a spin-stabilised disc, based on the standard equations of motion of a rigid flight vehicle in three dimensions (Etkin and Reid, 1996), was numerically simulated with inputs from the experimental data to allow the analyses of its trajectories, attitudes, and ranges. The implementation of these equations of motion into numerical simulation, coded in Matlab, were adapted from the work of Crowther and Potts (2007). Therein, the aerodynamic-gyroscopic coupling on the disc flight was simplified by first setting the disc's yaw rate (r) equal to the disc's spin rate (Ω), approximated to be a constant. The spinning of the disc, in turn, causes the disc to precess gyroscopiccally whereby its pitching moment is translated into a rolling (i.e., banking) motion. This precession happens when the spinning disc resists the torque applied as a pitching moment (M) perpendicular to the spinning axis, manifesting it instead into a rolling motion at an angular rate (p) in the axis perpendicular to both the spinning and the pitching axes. This gyroscopic relationship is expressed mathematically as

$$M = p \times I\Omega \qquad (1)$$

where (I) is the moment of inertia of the disc. Since rolling destabilizes the flight of a disc, reducing the magnitude of M for a given Ω improves the flight. The initial conditions of the simulation were set at fixed values: launch position, set at the origin (i.e., $x = y = z = 0$), speed (V_L) of 20 m/s, angle-of-attack (α_L) of 0^o, pitch angle (θ_L) of 15^o, and roll angle (ϕ_L) of 0^o. The advance ratio ($AdvR$),

$$AdvR = \frac{\Omega d}{2V_L} \qquad (2)$$

is fixed at 0.5 with a clockwise spin at launch to represent a typical value widely used by disc golf players (Potts, 2005). The simulated disc has a mass of 0.177 kg and a diameter (d) of 0.214 m.

Results

The experimental data are used to profile two flight parameters against α: the lift-to-drag ratio (C_L/C_D) and the pitching moment coefficient (C_M). The data is also used to extract the location of the aerodynamic centre (x_{ac}) of each disc, measured from its centre of gravity (c.g.).

The simulation extracts important properties during the flight of a disc, e.g., its coordinates, attitudes, angles-of-attack, and the range travelled. The simulation measures the ground range (i.e., the linear distance covered between launch to landing points) instead of the actual ground distance traced by the disc's trajectory.

Experiment: parametric discs

Figure 2a shows the profiles of C_L/C_D for the parametric discs with different cambers and the thicker flat disc as the baseline. The disc with a camber ratio of 1 (labelled with a triangle symbol) attains the highest C_L/C_D at all α, with a peak of 4.2 at $\alpha = 9^o$. The C_L/C_D values of both the flat and the negatively cambered (diamond symbol) discs are almost identical with a maximum of 2.4 across flatter peaks ranging from 7^o to 13^o; these values are lower than those of the positively cambered discs (except for α less than -3^o). The disc with a camber ratio of 0.25 (square symbol) has a maximum C_L/C_D value of 3.2 at 10^o. The C_M profiles for these discs (Figure 2b) show two key observations: (1) the gradients of all the profiles are positive, and (2) the trim conditions (i.e., $C_M = 0$) are near $\alpha = 0^o$, except for the negatively cambered disc, whose trim point (defined as the angle of attack for zero C_M [Potts, 2005]) is near $\alpha = -1^o$. Both the positively cambered discs exhibit the unfavourable behaviour of higher C_M values compared to those of the negatively cambered and flat discs.

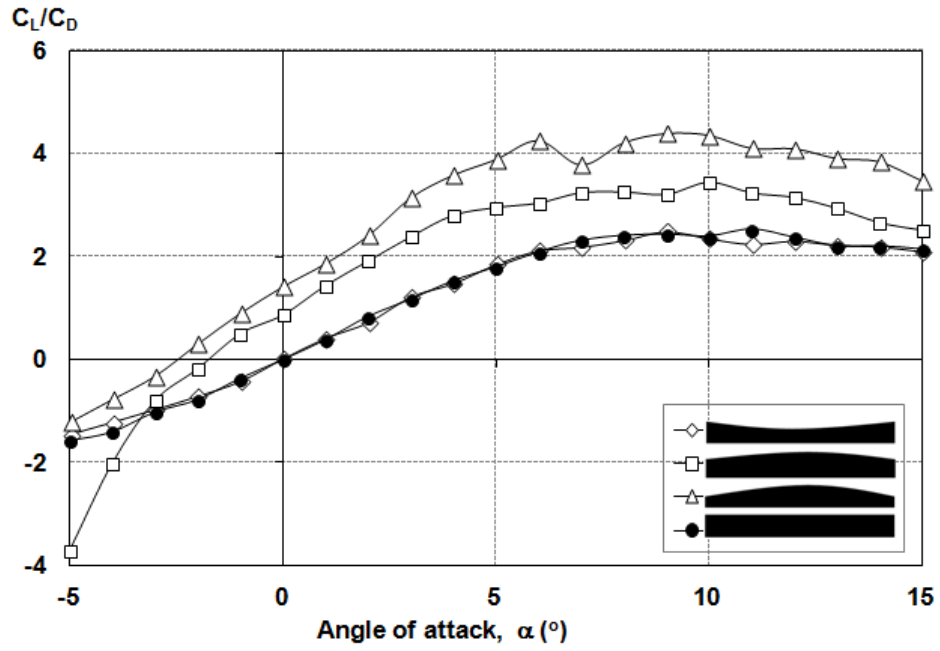

Figure 2a The effect of camber on C_L/C_D.

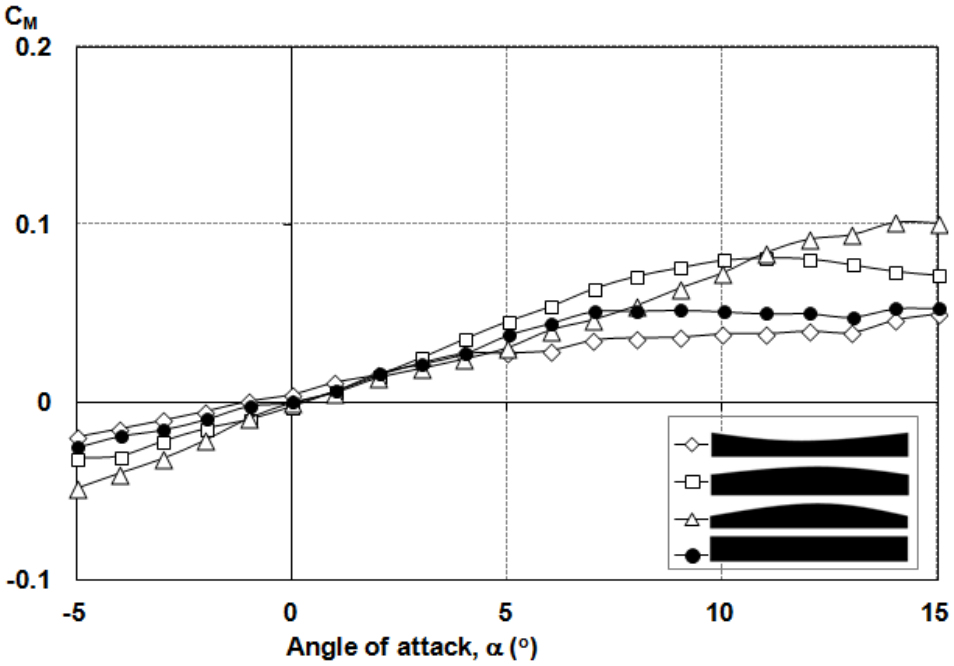

Figure 2b The effect of camber on C_M.

Figure 3a profiles the effect of cavity on the two flight parameters for a disc with cavity (h_o/t = 0.8), compared against those of the flat disc. At α = 0°, the C_L/C_D value is positive for the disc with cavity depth, with similar patterns afterward for both discs. This disc also exhibits the more favourable lower C_M magnitudes for a large range of α compared to those of the flat disc (Figure 3b). The gaps between these C_M magnitudes are significant for α between 6° and 11°. The disc with cavity is trimmed at α = 1°.

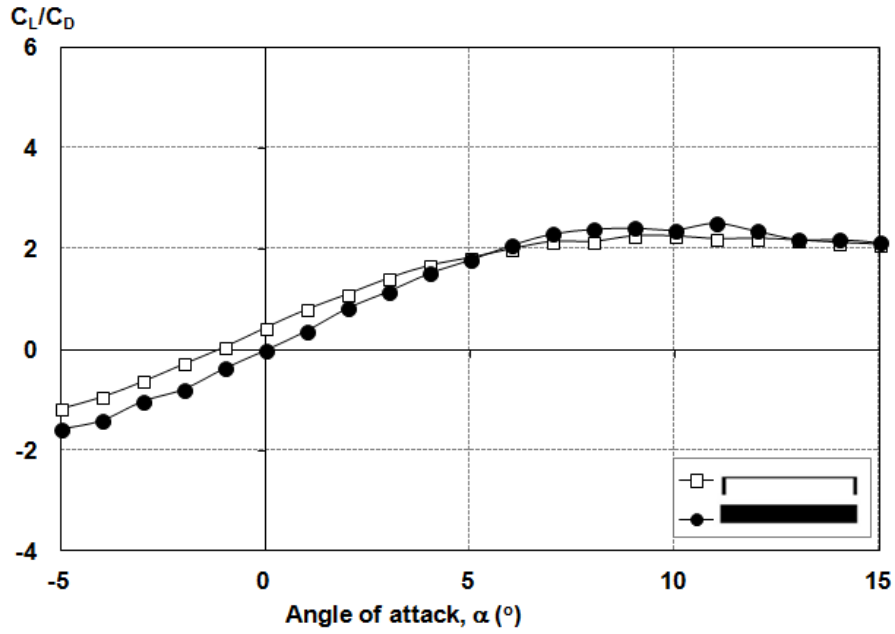

Figure 3a The effect of cavity on C_L/C_D.

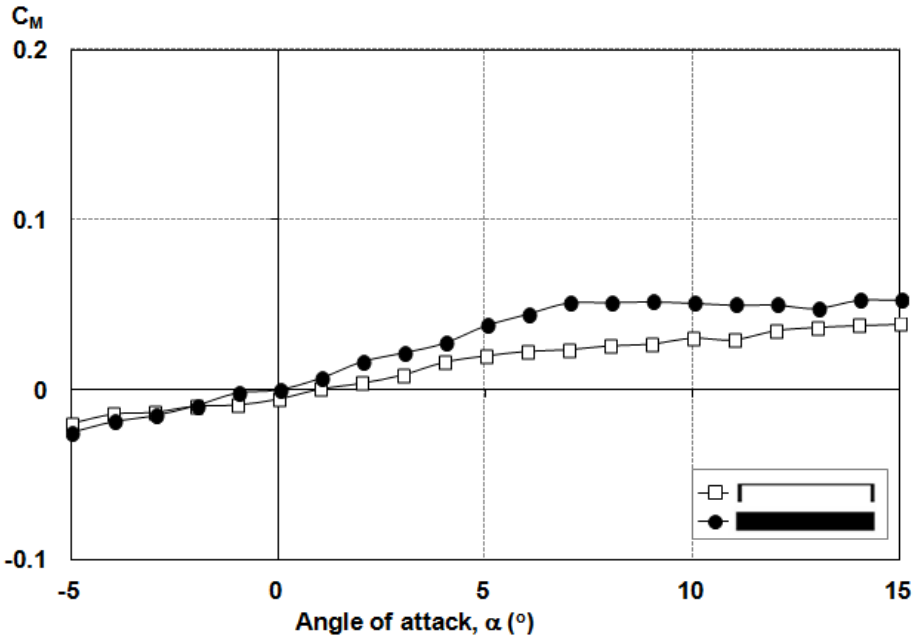

Figure 3b The effect of cavity on C_M.

The effect of rim geometry on the two flight parameters (Figure 4a) are profiled for four parametric discs with varying edge shapes: sharp, blunt, rounded, and square (i.e., the baseline flat disc). Favourable results of high C_L/C_D are shown by the discs with sharp and blunt edges (diamond and square symbols, respectively) due to the streamlining effect of these edges. C_L/C_D peaks at 5.0, 4.3, 3.3, and 2.5 for the sharp, blunt, rounded, and square edges, respectively. Conversely, C_M are more favourable (i.e., with lower magnitudes) at large α for the rounded and square edges (Figure 4b). All the discs are trimmed at $\alpha = 0^o$; beyond 7^o, C_M flattens off to around 0.05 for the flat disc.

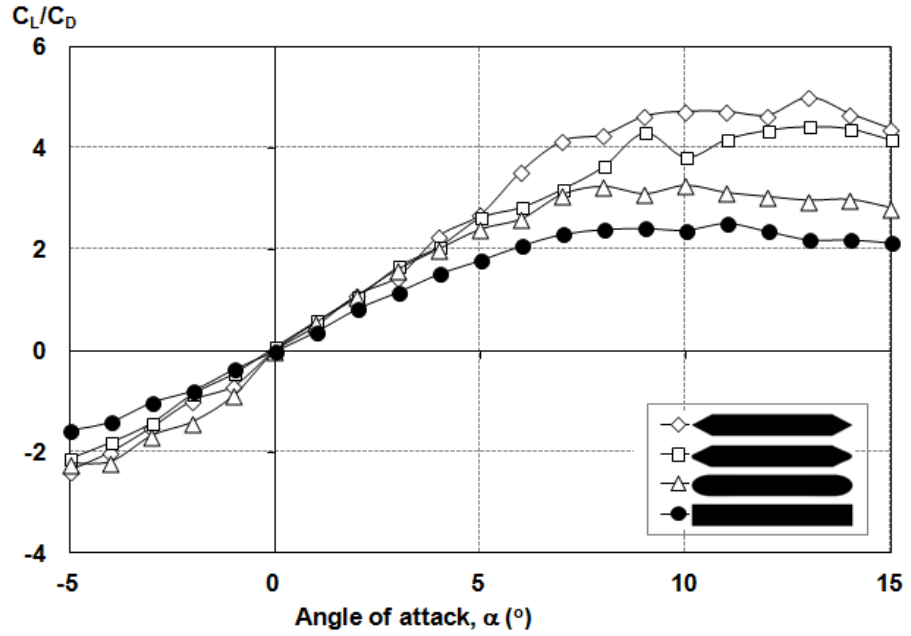

Figure 4a The effect of rim geometry on C_L/C_D.

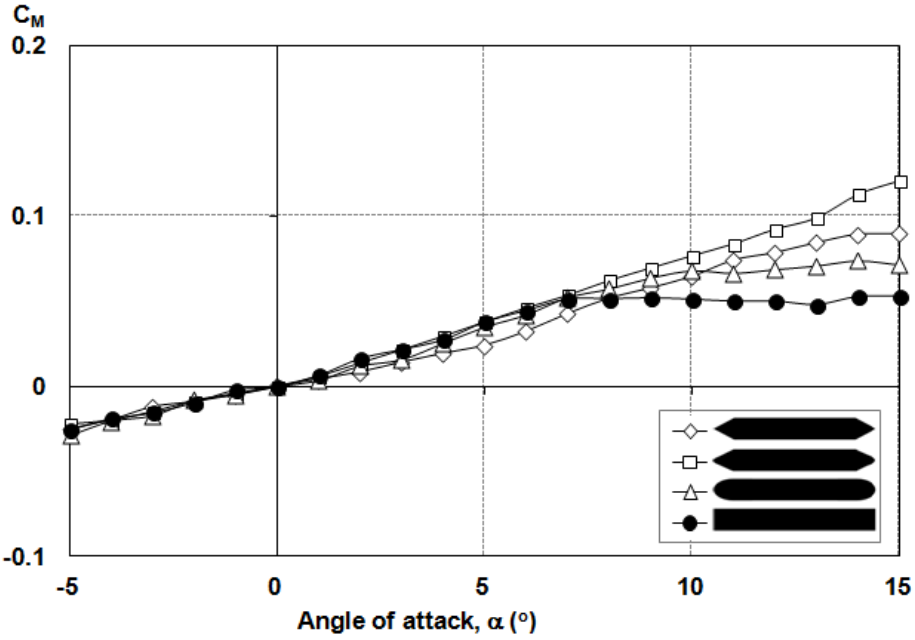

Figure 4b The effect of rim geometry on C_M

Experiment: golf discs

The profiles of the two flight parameters of the commercial golf discs are compared to those of the thinner flat disc in Figure 5a. At α = 0°, C_L/C_D are non-zero except for that of the flat disc; these values are 2.6, 1.8, 1.3, 0.8, and 0 for the driver, putter, Frisbee, mid-range, and flat discs, respectively. In addition, the C_L/C_D of these commercial discs increase

considerably for α between -5° up to about 3°. Owing to its small frontal area, thus reducing its pressure drag, the C_L/C_D gradient of the flat disc is the largest at 0.71/degree.

The flat disc attains a relatively sharp C_L/C_D peak of 5.3 at α = 8°, which declines afterward. The gradients of the other discs are lower, with flatter peaks of approximately 4.0, 3.3, 2.8, and for the driver, mid-range, putter, and Frisbee discs, respectively. The peaks for these discs are maintained over a large range of α from about 3° to 15°. The C_M gradient is positive (within its linear region) for each disc (Figure 5b), with a value of approximately 0.009/degree for the flat disc, followed by 0.007/degree (the driver disc), 0.003/degree (the mid-range disc), 0.002/degree (the putter disc), and 0.001/degree (Frisbee). The trim points are at α = 0° for the flat disc, 4° for the driver disc, and near 7° to 8° for the other two.

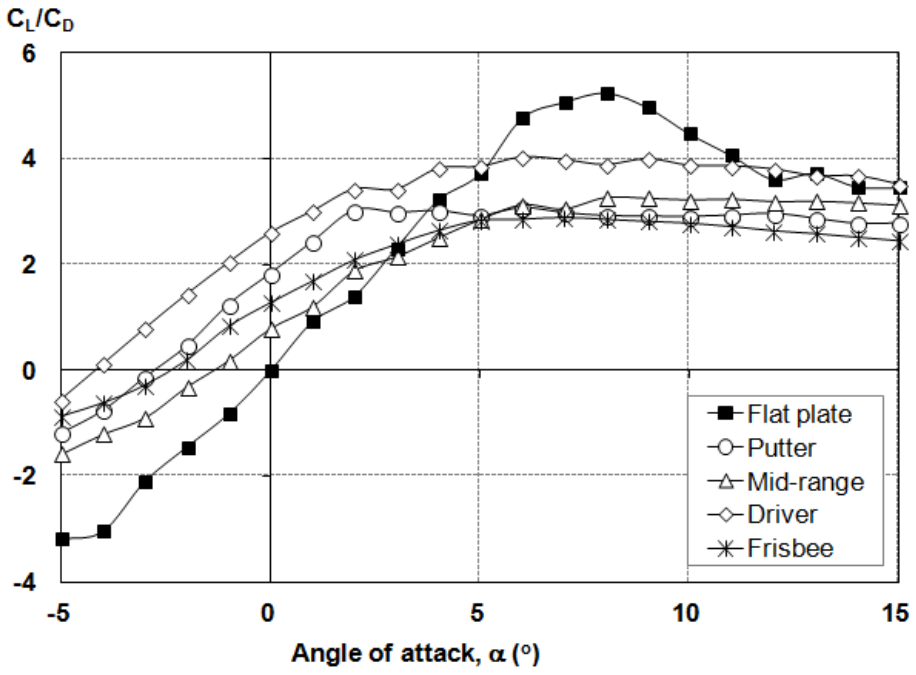

Figure 5a C_L/C_D comparison of the commercial golf discs

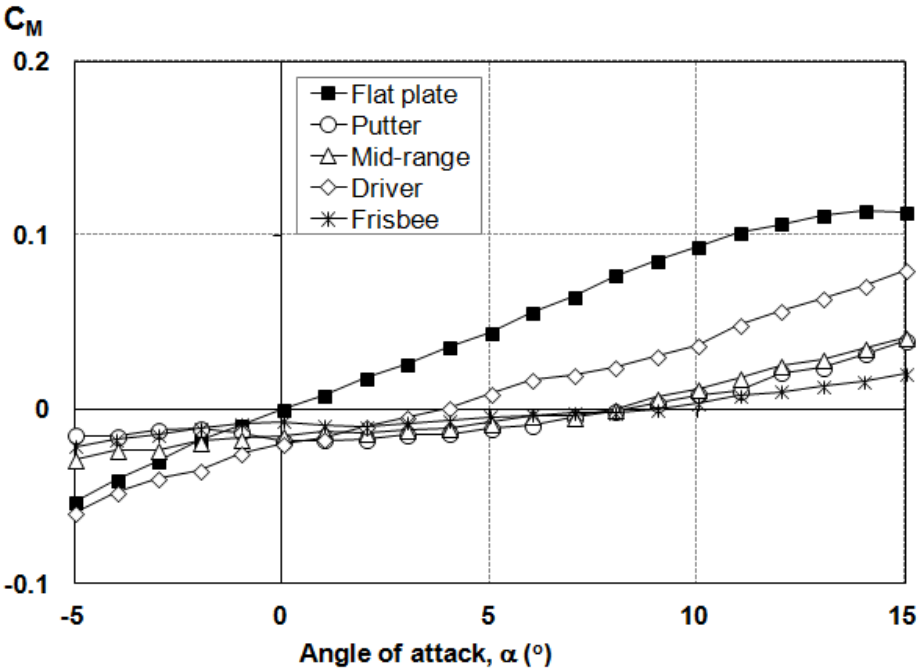

Figure 5b C_M comparison of the commercial golf discs.

Experiment: aerodynamic centre

The aerodynamic centre (x_{ac}) of a disc, measured relative to its c.g., is a point where its pitching moment coefficient ($C_{M,ac}$) remains approximately constant across a wide range of α, where

$$C_M = C_L \frac{x_{ac}}{d} + C_{M,ac} \qquad (3)$$

$$\frac{x_{ac}}{d} = \frac{\partial C_M / \partial \alpha}{\partial C_L / \partial \alpha} \qquad (4)$$

Eqn. (4) is consistent with the finding by Etkin and Reid (1996) that the pitcing moment gradient depends on x_{ac}. These locations, presented in Table 1, are computed based on the crude approximation of linearity for the gradients of C_M and C_L.

The centres of pressure (c.p.) of a disc (i.e., the location at which the aerodynamic lift and drag act) have also been extracted from the experimental data. Their normalized values, x_{cp}, measured relative to the centre of gravity of each disc are plotted in Fig. 6; only x_{cp} values for $\alpha > 0^o$ are focused due to their relevance to the simulated flights.

Table 1 Locations of discs' aerodynamic centres, ranked in the ascending order of magnitudes.

Discs	X_{ac}/d
Frisbee disc	0.03
Golf disc: Putter	0.05
Golf disc: Mid-range	0.07
Flat disc: *t/d* = 0.10	0.12
Golf disc: Driver	0.15
Flat disc: *t/d* = 0.01	0.21

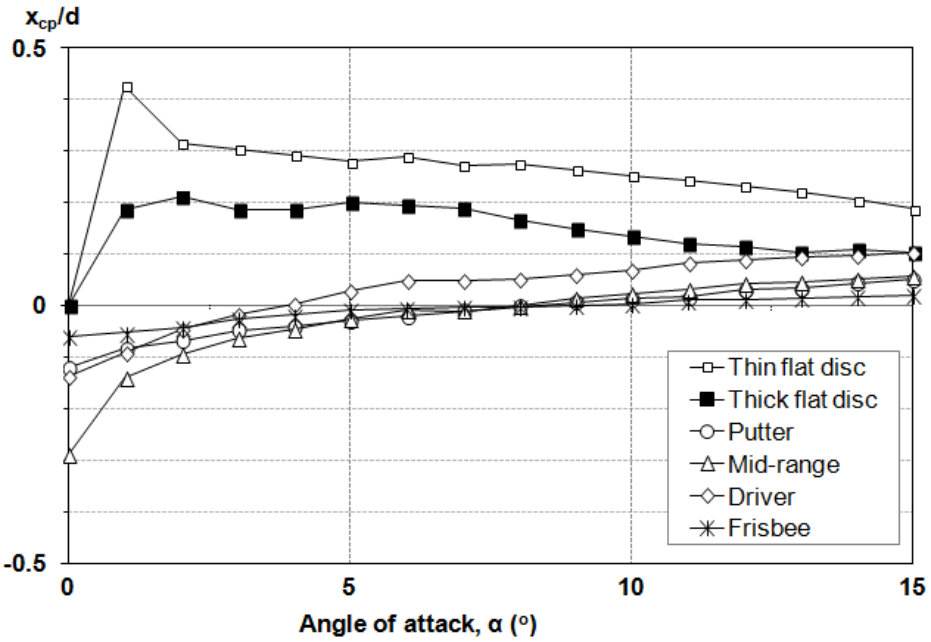

Figure 6 Location of X_{cp}/d for commercial golf discs.

Simulation

Flight trajectories originated from the launch position for the golf, Frisbee, and thin flat discs are mapped in the *XZ* (i.e., the side view, Fig. 7a) and *XY* (i.e., the top view, Fig. 7b) planes. The range (*R*) is defined as the linear ground distance between the launch and landing points, as extracted from Fig.7a. The driver disc attains the largest distance (with *R* = 63 m), followed by the mid-range (54 m), putter (49 m), Frisbee (48 m), and flat (35 m) discs.

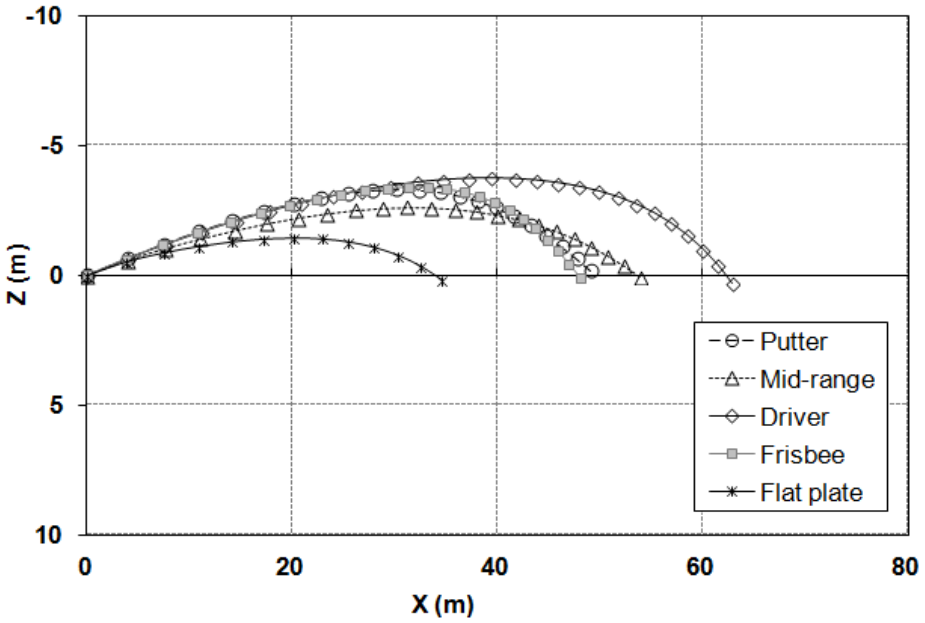

Figure 7a Golf disc flight trajectories in XZ plane.

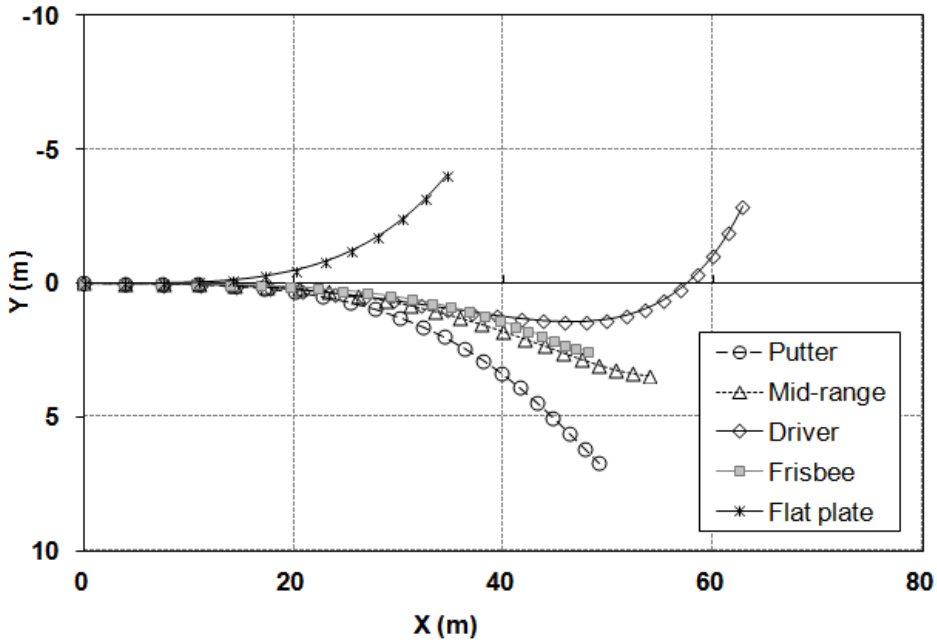

Figure 7b Golf disc flight trajectories in XY plane.

The top-view trajectory shows that the golf and Frisbee discs bank rightward (from the view of the thrower) immediately after the launch; these banking motions are consistent with the discs' negative C_M at lower α. Conversely, the flat disc banks leftward due to its positive C_M at lower α. Unlike the Frisbee and the other golf discs, the driver disc reverses its banking (i.e., lateral) direction mid-flight.

The dimensionless time (t') histories of the angle-of-attacks (α) and roll angles (ϕ) of the discs are tracked in Figs. 8a and 8b, respectively. t' is defined as the ratio between the actual and total flight times. All the discs experience

increasing α for most of their flight duration; α for the driver disc peaks near the end of its flight and decreases thereafter. The discs' roll angles (except that of the flat disc) also increase toward positive maxima, before decreasing toward negative values. ϕ for the flat disc, on the other hand, decreases toward negative values immediately after launch.

Discussion

To improve the flight performance of a disc in terms of its maximum range for a given launch speed, analogous to that of an aircraft, C_L/C_D should be maximized. On the other hand, the magnitudes of C_M at all α should be minimized to reduce rolling during the gyroscopic precession. The trim point of a disc is of particular importance: similar to that of an aircraft, the trim point has a major influence on the flight stability of a disc.

Performance of disc flight

Examining the angles-of-attack of the discs in Fig.8a, one key observation is that they vary during flight, mostly with increasing values from their initial conditions of 0^o at launch (except for that of the driver disc); this finding agrees with the work of Potts (2005). To achieve a stable flight, it is thus favourable for a disc to have constant flight parameters over the range of its operating α. Realistically however, variations of the two key flight parameters, C_L/C_D and C_M, depend on the type of disc. In the extreme case, the thin flat disc exhibits the largest gradients of both parameters, with a relatively sharp C_L/C_D peak. These properties in turn cause the disc to attain desired high lift only momentarily around α between 7^o to 9^o (as seen from Fig. 5a). Worse, it banks easily due to the rolling motion, or lateral instability, induced by the large C_M gradient; the high lift is in fact experienced during this rolling motion. In contrast, the putter and Frisbee discs have more favourable C_M with gradients at least four times smaller than that of the thin flat disc, but at the expense of lower C_L/C_D peaks.

Further examination of the rolling motion reveals another "mode" of lateral instability: lateral reversal, where the disc changes its lateral direction during flight (as seen in the flight path of the driver disc in Fig. 7b). This behavior is associated with the peak in the profile of the rolling attitudes of each disc (see Fig. 8b). The peak corresponds to a change of sign for the roll rate (p). This instantaneous point in flight occurs at the trim point of the disc, when its α during flight is examined in Fig. 5b. This change of the sign of p, in time, leads ϕ to change its sign (i.e., at $\phi = 0^o$), effectively switching the direction of the lateral force on the disc. This "switch" induces the disc to gradually reverse its lateral direction of flight, thereby tracing an "S-shaped" trajectory on the ground. In our simulation, only the driver disc remains in flight during this reversal. (The flights of the other discs could have been extended to include the lateral reversals by increasing their launch heights.)

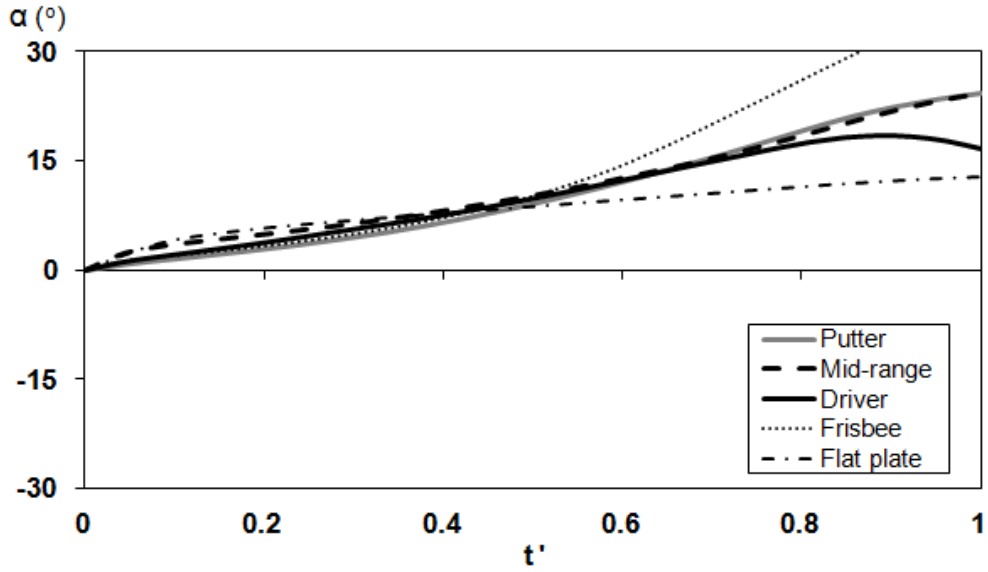

Figure 8a Attitude time histories with respect to angle of attack.

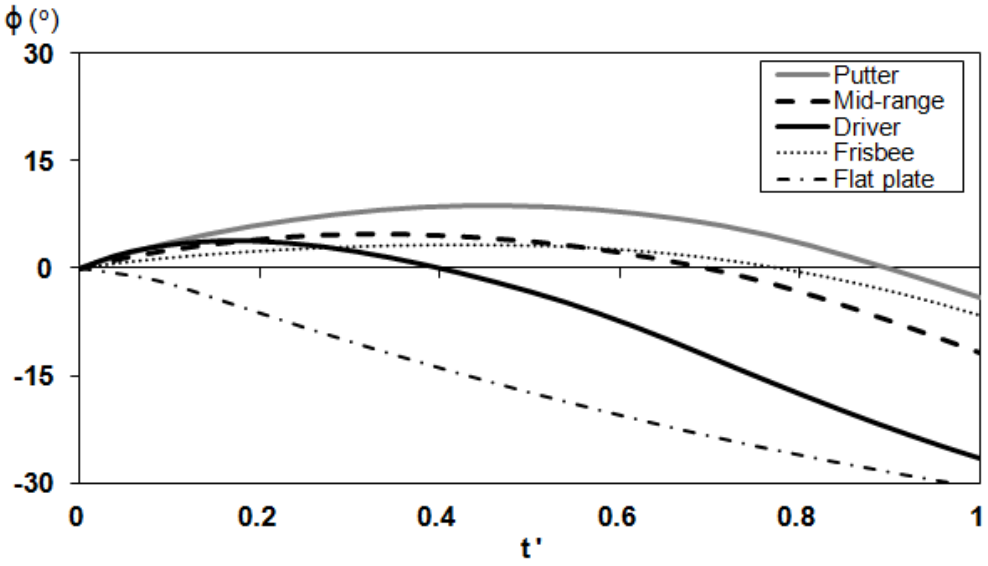

Figure 8b Attitude time histories with respect to roll angle.

These lateral instabilities of a flying disc are essentially induced by its pitching moment (C_M) that leads, gyroscopically, to an adverse roll (as described by Eq. (1)). This pitching moment is generated primarily by the aerodynamic lift acting at the disc centre of pressure. As such, an x_{cp} with a smaller magnitude (i.e., a centre of pressure nearer to the disc centre) is preferable as it reduces the moment-arm for the lift to produce the adverse pitch, and in turn, the adverse roll. The magnitudes of x_{cp} vary both with α and the type of disc (see Fig. 6). These results are consistent with the discussion on the lateral stability above: x_{cp} of the golf and Frisbee discs are closer to their centres of gravity (indicating more stable flights) compared to that of the flat disc.

However, x_{cp} is not a clear performance indicator on the lateral stability of a disc because of its variation with positive α. The aerodynamic centre, roughly invariant with α, is a more definitive, albeit simpler, choice in this respect. Table 1 ranks x_{ac} for the golf and flat discs; the order is similar to that extracted from the x_{cp} plots in Fig. 6, except for the reversed positions between the driver disc and the thicker flat disc (in such a case, the approximation of linearity to compute x_{ac} breaks down).

Considerations for disc design

Based on our data and simulation, a disc should be improved by (1) minimizing both its C_M magnitudes and gradient to reduce rolling, (2) shifting its trim point from the origin (i.e., $\alpha = 0^o$) to a positive α such that trimming is achieved mid-flight to minimize trajectory diversion, and (3) maximizing C_L/C_D with a flatter peak across a wide range of α to maximize the time for optimum flight.

The parametric data reveal that the best strategy to achieve a favourable C_M curve is by introducing a cavity into the lower surface of a disc, as evident in Fig. 3b, where its performance in this respect is better than that of the thicker flat disc. Another disc with a slightly better C_M curve than that of this baseline data is the negatively cambered disc (see Fig. 2b), which can be considered as having an "inverted" cavity, etched at the disc's upper surface. The disc with the sharp rim edge (see Fig. 4b) has lower C_M magnitudes, compared to those of the baseline data, at α of up to 7^o. Its C_M, however, continue to increase beyond this α, while those of the baseline disc flatten to approximately 0.05.

Similarly, the location of the trim point of a disc is also influenced by the cavity only. A lower-surface cavity increases the α of the trim point beyond 0^o (see Fig. 3b) and an upper-surface cavity reverses this shift (i.e. negative camber). The other design properties studied in this work, i.e., rim edge-shape, camber, and thickness, has no effect on shifting the trim point away from $\alpha = 0^o$.

One possible reason for this shift of the trim point for a disc with cavity is due to the flow separation underneath its cavity. At $\alpha = 0^o$, the flow separates from the front lip of the cavity, potentially reducing its pressure on the disc. On the other hand, the rear lip of the cavity, facing the flow, builds up the pressure nearby, resulting in a pitch-down moment. The flow separation gradually diminishes as α increases, resulting in a positive C_M gradient and a shifted trim-point.

From examination of our data, adding camber seems to offer the best option for optimizing the C_L/C_D curve (see Fig. 2a); the peak flattens for a wider range of α, compared to the outcomes of using the thicker flat disc or the other options (i.e., using cavity or more streamlined rims). Rim-streamlining alone does increase C_L/C_D peaks but reduce their ranges across α, relative to those of the thicker flat disc. Cavity does not offer any substantial improvement on C_L/C_D compared to the baseline data of the thicker flat disc.

In addition to the design recommendations above, Eq. (1) offers another approach to reduce the lateral instability caused by the gyroscopic effect. For the same pitching moment, the rolling motion of a disc can be reduced by increasing its moment of inertia (I). One way to increase I is by distributing the mass of the disc away from its centre. A good illustration of this practice is the design of the ringed Aerobie^{TM} disc (Cassidy, 1990).

For the golf discs, the performance of the putter and Frisbee discs is optimized by minimizing pitch; the performance of the driver disc, on the other hand, is optimized by maximizing its C_L/C_D, at the expense of increasing its C_M gradient. These optimizations produce, as simulated, a putter and Frisbee discs with straighter but shorter path, and a driver disc that can be thrown farther but with a higher tendency to yaw from its intended path.

Conclusion

This work has examined the effect of design parameters on the performance of flying sports discs. Experiments and simulations performed on selected sets of parametric and commercial golf discs revealed two key performance parameters to evaluate the flight performance of a disc: its coefficient of lift-to-drag ratio and, more importantly, its coefficient of pitching moment. The C_M describes the pitching moment coefficient which eventually influences its tendency to yaw throwing distance in terms of sensitivity at launch. For optimum performance, the magnitudes and gradient of its C_M should be minimized and its trim-point shifted from $\alpha = 0^o$, while its C_L/C_D should be maximized with a flatter peak. Data from this study supports the explanation for the well-known "S-shaped" trajectory traced by a flying disc. The lateral reversal during flight (thus producing the "S" shape) is induced when the disc achieves its trim point, causing its pitching moment to change sign. Simultaneously, its rolling direction is reversed as well due to the coupling effect produced by the gyroscopic precession.

One unexplored issue in this work is on the variation of the discs' angles-of-attack during flight. In our simulation, α increases over time for each disc; with it, the disc's flight characteristics and attitudes vary as well. A disc with a more controlled flight (i.e., one that follows its intended path) could be thrown if its α is maintained during flight, or confined to small changes only. Understanding the cause of this variation is crucial to lead to better and more targeted design changes on a disc.

References

Asai, T., Seo, K., Kobayashi, O. and Sakashita, R. (2007). Fundamental aerodynamics of the soccer ball. *Sports Engineering,* Vol. 10 No. 2, pp. 101–110. doi: 10.1007/BF02844207.

Cassidy, J. (1990). *The Aerobie Book: An investigation into the Ultimate Flying Mini-Machine*, Klutz Press.

Crowther, W.J. and Potts, J.R. (2007). Simulation of a spin stabilized sports disc. *Sports Engineering*, Vol. 10 No. 1, pp. 3-21. doi: 10.1007/BF02844198.

Etkin and Reid. (1996). *Dynamics of flight: Stability and Control*, Wiley.

Haake, S.J., Goodwill, S.R. and Carre, M.J. (2007). A new measure of roughness for defining the aerodynamic performance of sports balls. *Proceedings of the Institution of Mechanical Engineers, Part C: Journal of Mechanical Engineering Science*, Vol. 221 No. 7, pp. 789-806. doi: 10.1243/0954406JMES41.

Higuchi, H., Goto Y., Hiramoto, R. and Meisel, I. (2000). *Rotating Flying Disks and Formation of Trailing Vortices*, 18th AIAA Applied Aerodynamics Conference, Denver, CO, USA. doi:10.2514/6.2000-4001.

Hughes M.D. and Bartlett R.M. (2002). The use of performance indicators in performance analysis. *Journal of Sports Sciences*, Vol. 20 No. 10, pp. 739-754. doi: 10.1080/026404102320675602 .

Hughes, M.D. (2004). Performance analysis: A mathematical perspective. *International Journal of Performance Analysis Sport*, Vol. 4 No. 2, pp. 97 – 139.

Hummel S. and Hubbard M. (2001). *A Musculoskeletal Model for the Backhand Frisbee Throw*. 8th International Symposium on Computer Simulation in Biomechanics, Milan, Italy.

James, D. and Haake, S. (2008). The spin decay of sports balls in flight (P172). *The Engineering of Sport*, Vol. 7 No. 2, pp. 165- 170. doi: 10.1007/978-2-287-09413-2_20.

Lissaman, P. (1998). *Disc Flight Dynamics*. Unpublished manuscript. The University of Southern California, USA.

Lissaman P. and Hubbard M. (2010). Maximum range of flying discs. *Procedia Engineering*, Vol. 2 No. 2, pp. 2529-2535. doi:10.1016/j.proeng.2010.04.027.

Nevill, A.M., Atkinson, G. and Hughes, M.D. (2008). Twenty-five years of sport performance research in the Journal of Sports Sciences. *Journal of Sports Sciences*, Vol. 26 No. 4, pp. 413- 426. doi: 10.1080/02640410701714589.

Passmore, M.A., Tuplin, S. Spencer, A. and Jones, R., (2008). Experimental studies of the aerodynamics of spinning and stationary footballs, *Proceedings of the Institution of Mechanical Engineers, Part C: Journal of Mechanical Engineering Science*, Vol 222 No. 2), pp. 195-205. doi: 10.1243/09544062JMES655.

Potts J.R. and Crowther W.J. (2001). *Flight Control of a Spin Stabilised Axi-symmetric Disc-wing*, AIAA 2001-0253, 39th Aerospace Sciences Meeting & Exhibit, Reno, NV, USA. doi: 10.2514/6.2001-253.

Potts J.R. and Crowther W.J. (2002). *Frisbee™ Aerodynamics*, AIAA 2002-3150, 20th AIAA Applied Aerodynamics Conference & Exhibit, St. Louis, MI, USA. doi: 10.2514/6.2002-3150.

Potts, J. R., (2005). *Disc-wing Aerodynamics*. PhD Thesis, University of Manchester, UK.

Wesson, J. (2009). *The Science of Golf*, Oxford University Press, UK.